Influence of External Factors on the Micellization Process and Aggregate Structure of Poly(oxy)styrene−Poly(oxy)ethylene Block Copolymers

Emilio Castro,[†] Silvia Barbosa,[†] Josué Juárez, Pablo Taboada,*[,†] Issa A. Katime,[‡] and Víctor Mosquera[†]

Grupo de Física de Coloides y Polímeros, Grupo de Sistemas Complejos, Departamento de Física de la Materia Condensada, Facultad de Física, Universidad de Santiago de Compostela, Santiago de Compostela, Spain, and Grupo de Nuevos Materiales y Espectroscopia Supramolecular, Departamento de Química-Física, Facultad de Ciencia y Tecnología, Campus de Leioa, Universidad del País Vasco, Apartado 644, Bilbao, Spain

Received: November 29, 2007; In Final Form: January 31, 2008

Solutions of the polyoxystyrene−polyoxyethylene block copolymer $SO_{17}EO_{65}$, where SO denotes polystyrene oxide block as the hydrophobic block and EO the polyethylene oxide block as the hydrophilic block, in mixtures of water (a selective solvent for the EO blocks) and 1,4-dioxane (a good solvent for both blocks) were studied by surface tension and light scattering measurements. Surface and micellar structural parameters have been analyzed as a function of solvent composition. The critical micelle concentration increases and the micellar aggregation number decreases, respectively, as the amount of 1,4-dioxane in the binary solvent increases as a consequence of the enhanced solubility of the SO blocks in the solvent mixture, causing the lowering of the interfacial tension between the hydrophobic blocks in the micellar core and the solvent; therefore, to achieve thermodynamic equilibrium, the micelle size decreases. In addition, static light scattering (SLS) has been proved to be a useful technique to detect the lower boundary of the transition between a dilute micellar solution (sol) to a local-ordered micellar solution (soft gel) resulting from a percolation mechanism. Comparison of the sol−soft gel boundaries obtained from SLS for copolymers $SO_{17}EO_{65}$ and $EO_{67}SO_{15}EO_{67}$ with those previously derived by rheology is made. Finally, changes in the autocorrelation function of the solutions at the boundary obtained from dynamic light scattering are also analyzed.

Introduction

Polyoxyalkylene amphiphilic block copolymers containing both polyoxyethylene hydrophilic block and different hydrophobic blocks can form self-assembled aggregates when dissolve in selective solvents (good solvent for one block and poor solvent for the other constituting blocks), from spherical micelles in dilute solutions to lyotropic liquid crystals in the concentrated regime.[1] These micelles consist of a compact swollen core of insoluble blocks surrounded by a highly swollen corona of the water-soluble polyoxyethylene blocks. This behavior provides the great utility of this type of materials in different industrial applications such stabilizers, thickeners, foaming agents, and emulsifiers.[2] Their properties can be adjusted to meet the specific requirements of a particular application by changing the synthetic parameters, that is, the copolymer architecture, block nature, block lengths, or copolymer molecular weight,[3] or by changes in the conditions of the surrounding environment of the block copolymer, such as the temperature, ionic strength, solvent type, and the presence of cosolutes.[4] Depending on the particular needs, one or both approaches can be used, although the first one usually takes a longer time since it demands the synthesis of new polymeric molecules. Due to this, in the past decade, a great effort has been devoted to the study of the physicochemical properties and mesophase formation of different polyoxyethylene-based block copolymers under different solution conditions, mainly on those whose hydrophobic block is formed by propylene oxide (denoted as PO), known as Pluronics. Solvent quality has been shown to be a key factor in controlling the critical micelle concentration (cmc), critical micelle temperature (cmt), and micelle and mesophase structure. This solvent quality can be modified by changes in temperature[2,5,6] and the addition of cosolutes[7−9] and cosolvents.[10−13] However, less attention has been paid to other polyoxyethylene-based block copolymers with hydrophobic blocks composed of butylene oxide (BO) or styrene oxide (SO).[14−16]

Thus, in the present work, we analyze by static and dynamic light scattering the micellization properties of the diblock copolymer $SO_{17}EO_{65}$ in mixed solvents formed by water (a selective solvent for PEO blocks (OCH_2CH_2)) and 1,4-dioxane (a nonselective solvent) with different proportions of the components. The subscripts indicate the block lengths, and SO represents the styrene oxide unit ($-OCH_2CH(C_6H_5)$). The synthesis and micellization properties in pure water of this block copolymer at different temperatures have been previously reported.[17,18] In general, the addition to water of a cosolvent provides an extra degree of freedom in tailoring the solution properties. In this regard, previous studies have shown that the different proportions of both solvents in the mixture gives rise to different self-assembled polymeric structures,[19,20] in particular for polyoxystyrene−polyoxyethylene (PSO−PEO) copolymers where polymeric crew-cut micelles and vesicles are observed,[21,22] and regulates the ion flux through vesicle membranes,[23] depending on the cosolvent proportion in the mixed solvent, all of which can be really useful for specific applications

* To whom correspondence should be addressed: E-mail: fmpablo@usc.es. Tel: 0034981563100, Ext 14042. Fax: 0034981520676.
[†] Universidad de Santiago de Compostela.
[‡] Universidad del País Vasco.

10.1021/jp7112895 CCC: $40.75
Published on Web 04/08/2008

TABLE 1: Molecular Characteristics of the Copolymers[a]

	M_n/g mol^{-1} (NMR)	wt % SO (NMR)	M_w/M_n (GPC)	M_w/g mol^{-1}
$SO_{17}EO_{65}$	4940	42.1	1.04	5140
$EO_{67}SO_{15}EO_{67}$	7700	23.0	1.04	8100

[a] Estimated uncertainty: M_n to ±3%; wt % S to ±1%, M_w/M_n to ±0.01. M_w calculated from M_n and M_w/M_n.

such as in pharmaceutical and cosmetic formulations,[24] and ink-jet printing.[25]

It has been shown that the lower glass transition of poly(styrene oxide) ($T_g \approx 40$ °C) compared to polystyrene, denoted as PSt, ($T_g \approx 100$ °C) means that effects caused by immobility of blocks in the micelle core are less important in micellar solutions of these class of copolymers, giving rise to a very different solution behavior and structures in solution for St−EO and SO−EO copolymer with similar block lengths, and providing sufficient mobility to readily solubilize aromatic drugs to the latter.[17,26]

On the other hand, in the present work, we also show changes in polymer solutions under heating through static light scattering (SLS) and dynamic light scattering (DLS) with the previously established phase diagram of $SO_{17}EO_{65}$ and $EO_{67}SO_{15}EO_{67}$ derived by rheometry measurements. To the best of our knowledge, this is the first time that such correlation is established.

Experimental Section

Materials. The synthesis of the copolymers was described previously in detail.[17] Table 1 shows the molecular characteristics of both copolymers. Water was double distilled and degassed before use. 1,4-Dioxane was of spectroscopic grade.

Surface Tension Measurements. Surface tensions (γ) of the diblock copolymer $SO_{17}EO_{65}$ were measured by the Wilhelmy plate method using a Krüss K-12 surface tension equipment, equipped with a processor to acquire the data automatically. The equipment was connected to a circulating water bath to keep the temperature constant at 20 °C to within ±0.01 °C. The plate was cleaned by washing with doubly distilled water followed by heating in an alcohol flame. A stock solution (1.0 g dm^{-3}) was prepared with distilled water and diluted as required. To measure, a solution was equilibrated at 20 °C and the surface tension was recorded at 15-min intervals until a constant value was reached, a process that took 12−36 h depending on concentration. The accuracy of measurement was checked by frequent determination of the surface tension of pure water.

Light Scattering Measurements. DLS and SLS intensities were measured for solutions at 20 °C by means of a Malvern 7027 laser light scattering instrument with vertically polarized incident light of wavelength $\lambda = 514$ nm supplied by a 2-W argon ion laser supplied by Coherent Inc. combined with a Brookhaven Bi 9000AT digital correlator with a sampling time of 25 ns to 40 ms (for DLS). The intensity scale was calibrated against scattering from benzene. Measurements were made at scattering angle $\theta = 90°$ to the incident beam, as appropriate for particles that are smaller that the wavelength of light. Solutions were equilibrated at each chosen temperature for 30 min before making a measurement. Experiment duration was in the range 3−5 min, and each experiment was repeated two or more times. All solutions were optically clear to the eye. They were clarified by filtering through Millipore Millex filters (Triton-free, 0.22-μm porosity) directly into the cleaned scattering cell.

The correlation functions from DLS were analyzed by the CONTIN method to obtain intensity distributions of decay rates (Γ).[27] The decay rate distributions gave distributions of apparent diffusion coefficient ($D_{app} = \Gamma/q^2$, $q = (4\pi n_s/\lambda)\sin(\theta/2)$, with n_s the refractive index of solvent) and integrating over the intensity distribution gave the intensity-weighted average of D_{app}. Values of the apparent hydrodynamic radius ($r_{h,app}$, radius of hydrodynamically equivalent hard sphere corresponding to D_{app}) were calculated from the Stokes−Einstein equation

$$r_{h,app} = kT/(6\pi\eta D_{app}) \quad (1)$$

where k is the Boltzmann constant and η is the viscosity of water at temperature T.

The basis for analysis of SLS was the Debye equation

$$K^*c/(I - I_s) = 1/M_{w-} + 2A_2c + ... \quad (2)$$

where I is intensity of light scattering from solution relative to that from benzene, I_s is the corresponding quantity for the solvent, c is the concentration (in g dm^{-3}), M_w is the mass-average molar mass of the solute, A_2 is the second virial coefficient (higher coefficients being neglected), and K^* is the appropriate optical constant, which includes the specific refractive index increment, dn/dc. Other quantities used were the Rayleigh ratio of benzene for vertically polarized light, $R_v = 3.20 \times 10^{-5}[1 + 3.68 \times 10^{-3}(t - 25)]$ cm^{-1} (t in °C)[28] and the refractive index of benzene,[29] $n = 1.5131[1-6.4 \times 10^{-4}(t - 20)]$. The possible effect of the different refractive indices of the blocks on the derived molar masses of micelles has been considered for EO_mSO_n copolymers and found to be negligible.[30] The refractive index increments, dn/dc, of the block copolymer in the mixed solvents were measured at 20.0 ± 0.1 °C using a Brice-Phoenix differential refractometer operating at 532 nm, previously calibrated with solutions of highly purified NaCl, using a Nb:Yag laser as light source.

Rheometry. Sol−soft gel boundaries of solutions of copolymers $SO_{17}EO_{65}$ and $EO_{67}SO_{15}EO_{67}$were determined using a Bohlin CS10 rheometer with water bath temperature control. Couette geometry (bob, 24.5 mm diameter, 27 mm height; cup, 26.5 mm diameter, 29 mm height) was used, with 2.5 cm^3 of sample being added to the cup in the mobile state. A solvent trap maintained a water-saturated atmosphere around the cells, and evaporation was not significant for the temperatures and time scales investigated. Temperature scans were recorded for selected copolymer concentrations at a frequency $f = 1$ Hz. The samples were heated at ~1 °C min^{-1} in the range 5−85 °C. The strain amplitude (A) was not closely controlled during the T scans, and the changes in modulus were used only to indicate the temperatures at which soft gel formed and dispersed. A solvent trap maintained a water-saturated atmosphere around the cells. Frequency scans of storage (G') and loss (G'') moduli were recorded for selected copolymer concentrations and temperatures with the instrument in oscillatory shear mode and with the strain amplitude maintained at a low value ($A < 0.5\%$) by means of autostress facility of the Bohlin software. This ensured that measurements of G' and G'' were in the linear viscoelastic region.

Results and Discussion

Cosolvent Effect on the Surface Properties. Since the cmc of the block copolymer $SO_{17}EO_{65}$ in water is extremely low to obtain reliable values, a plot of log[cmc/(mol dm^{-3})] of experimentally measured cmc values against hydrophobic block length for other diblock SO copolymers with similar EO block

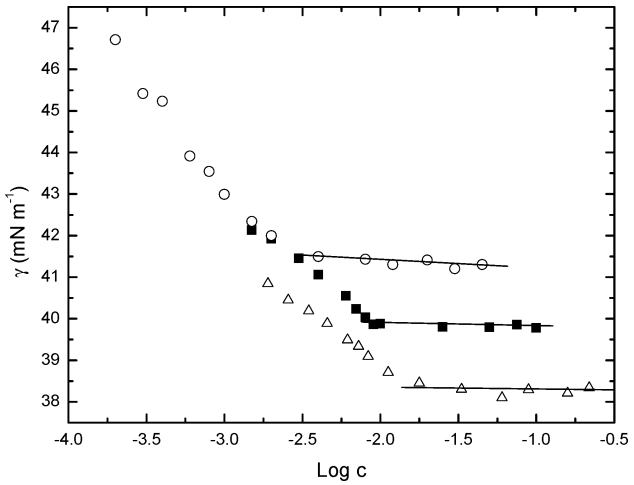

Figure 1. Surface tension of copolymer $SO_{17}EO_{65}$ in water−dioxane solvent mixtures containing (○) 20, (■) 30, and (△) 40% (v/v) 1,4-dioxane.

length by different SO length provides a satisfactory empirical relationship to derive approximated cmc values for copolymer of the same structure and block composition.[31] In this case, a value of ~0.0017 g dm^{-3} is obtained. The cmc values for the copolymer were still too low in the presence of small amounts of 1,4-dioxane to be measured with reasonable confidence. Nevertheless, in order to get an idea about the extent of micellization of the present diblock copolymer in water−dioxane solvent mixtures, we have performed surface tension measurements of this copolymer at 1,4-dioxane contents of 20, 30, and 40% (v/v). Representative plots showing several results of these experiments are presented in Figure 1. The concentration at which the surface tension departs from a steady value served to define the cmc. Values are shown in Table 2, from which a higher cmc is obtained as the 1,4-dioxane content in the mixed solvent increases. This indicates that the 1,4-dioxane−water mixed solvent becomes a better solvent for the copolymer than pure water. Therefore, the larger cmc values as the content of 1,4-dioxane increases indicate that the cosolvent is acting as a structure-breaking agent, decreasing the solvophobic effect and favoring the solution of the copolymer in the mixed solvents.

According to the mass action model the standard Gibbs energy of micelle formation per mole of monomer, ΔG^0_{mic}, is given by

$$\Delta G^0_{mic} = RT \ln x_{cmc} \tag{3}$$

where x_{cmc} is the mole fraction of copolymer at the cmc. The effect of the cosolvent on the micelle aggregation process can be evaluated by means of the so-called Gibbs free energy of transfer, ΔG^0_M,

$$\Delta G^0_M = (\Delta G^0_{mic})_{ethanol+water} - (\Delta G^0_{mic})_{water} \tag{4}$$

which is defined by The thermodynamic parameters obtained through eqs 3 and 4 are also listed in Table 2. It is observed that the Gibbs energies of micellization are negative but become lower (in absolute values) as the dioxane content increases. This indicates that the micellization process becomes less spontaneous with the presence of the cosolvent and reflects the role of the 1,4-dioxane reducing the solvophobic effect, which is considered to be responsible for the micellar formation process as a consequence of the reduction of solvent cohesive energy. Thus, the chemical structure of the solvent plays an important role in the cohesive energy density. This arises from the fact that in water solution the SO block is tightly coiled in the dispersed molecular state, so that its interaction with water is diminished, and the micellization process of long-SO block copolymers can be assumed safely as entropy driven. However, the progressive addition of 1,4-dioxane to the solution allows the solvent mixture to be a better solvent for the SO blocks, so the cosolvent is acting as a water structure breaker since its presence disrupts the hydrogen bond network of water, which results in a lesser dense coiled packing of these blocks. Nevertheless, it is necessary to bear in mind that, at very low cosolvent contents (less than 10% (v/v)), 1,4-dioxane stabilizes the water structure.[32] On the other hand, it has been shown that water−dioxane mixtures with dioxane content below 35% (v/v) are composed of mainly water associates and water−dioxane complexes, reflecting strong water−water and extensive intermolecular water−dioxane interactions, which alter water structure.[33] At higher dioxane contents up to 75% (v/v), small clusters of water−dioxane molecules are formed through hydrogen bonding.[33] All this involves a presumably increase in the values of the enthalpy of micellization and, therefore, of the enthalpic contribution to ΔG^0_{mic}. In addition, the values of the free energy of transfer are positive and increase with the 1,4-dioxane content. In particular, the magnitude of the polymer chain-transfer Gibbs energy is smaller in pure 1,4-dioxane than in water, and this is the dominant contribution responsible for the observed increase in the cmc as the cosolvent content in the solvent mixture increases.

On the other hand, the surface excess concentration, Γ_{max}, and the minimum area per copolymer molecule, A_{min}, at the air/solvent interface were obtained using the surface tension measurements and the following equations:

$$\Gamma_{max} = -\frac{1}{RT}\left(\frac{\partial g}{\partial \ln c}\right)_{T,p} \tag{5}$$

$$A_{min} = 1/N_A\Gamma_{max} \tag{6}$$

where R is the gas constant, N_A is the Avogadro's number, and c is the copolymer concentration. The values of the surface pressure at the cmc, π_{cmc}, were obtained employing the following equation:

$$\pi_{cmc} = \gamma_0 - \gamma_{cmc} \tag{7}$$

The Gibbs free energy of adsorption were obtained through[34]

$$\Delta G^0_{ads} = \Delta G^0_{mic} - \pi_{cmc}/\Gamma_{max} \tag{8}$$

The standard state in the surface phase is defined as the surface covered with a monolayer of copolymer at the surface pressure equal to zero. The last term in eq 8 expresses the work involved in transferring the polymer molecule from a monolayer at zero surface pressure to the micelle. The values of these surface quantities are also shown in Table 2. In the presence of 1,4-dioxane, values of Γ_{max} decreases with increasing dioxane content in the measured range. This decrease can be attributed to several factors: (a) a change in the water structure due to the addition of cosolvent, (b) the interaction dioxane−copolymer, and (c) the presence of 1,4-dioxane in the interface.[35] π_{cmc} also decreases with increasing 1,4-dioxane concentration in the mixed solvent. An increase in the 1,4-dioxane concentration results in a decrease in the dielectric constant, in the Reichardt parameter, E_T, or in the π^* polarity index[36] of the mixture,

TABLE 2: Critical Micelle Concentration, Gibbs Free Energy of Micelle Formation, ΔG^0_{mic}, Gibbs Free Energy of Transfer, ΔG^0_M, Surface Excess Concentration, Γ_{max}, Minimum Area Per Molecule, A_{min}, Surface Pressures, and Gibbs Energy of Adsorption, ΔG^0_{ads} of the $SO_{17}EO_{65}$ Block Copolymer in Different Aqueous−Dioxane Mixed Solvents at 20 °C[a]

% (v/v)	cmc (g dm^{-3})	ΔG^0_{mic} (kJ mol^{-1})	ΔG^0_M (kJ mol^{-1})	Γ_{max} (10^{-6} mol m^{-2})	A_{min} (nm^2)	π_{cmc} (mN m^{-1})	ΔG^0_{ads} (kJ mol^{-1})
20	0.003	−44.8	1.3	1.94	0.9	41.5	−66.2
30	0.009	−42.1	4.0	1.20	1.4	39.9	−75.4
40	0.025	−39.6	6.5	1.0	1.6	38.1	−87.7

[a] Estimated uncertainties: cmc, ΔG^0_{mic}, ΔG^0_M, Γ_{max}, A_{min} to ±10%, π_{cmc} to ±1%, smf ΔG^0_{ads} to ±15%.

this confirming that the bulk phase will be a better solvent for the polymer molecules and their tendency to be adsorbed at the interface will decrease. As a consequence, the surface excess concentration diminishes and the minimum area per molecule at the air/mixture interface increases upon increasing the amount of dioxane in the solvent mixture. Moreover, the values of ΔG^0_{ads} become more negative, probably indicating a dehydration of the polyoxyethylene units due to the presence of cosolvent molecules.

Cosolvent Effect on the Micellar Properties. We have performed light scattering experiments at sufficiently high copolymer concentrations to ensure that full micellization is achieved for the different compositions of the mixed solvents to allow the measurements of the micelle size. Intensity fraction distributions of decay times from DLS measurements obtained for copolymers $SO_{17}E_{65}$ contained narrow peaks that were assigned to spherical micelles formed by a closed association process. The decay time distribution of copolymer micelles in mixed solvents slightly widens and left-shifts as the 1,4-dioxane content in the solvent increases, as seen in Figure 2. This is the first indication that as the proportion of the cosolvent in the mixed solvent increases, smaller particles are present in the solution since the relaxation time becomes faster.

By integration of the intensity fraction distributions of decay times, the apparent diffusion coefficient is an increasing linear function of the copolymer concentration. The positive slopes of the plots of Figure 3 are consistent with the micelles acting effectively as hard spheres. This behavior is usually accommodated by introducing a diffusion second virial coefficient (k_d) in the equation of the straight line

$$D_{app} = D(1 + k_d c + ...) \quad (9)$$

The coefficient k_d is related to the thermodynamic second virial coefficient A_2 by[37]

$$k_d = 2A_2M_w - k_f - 2\upsilon \quad (10)$$

where k_f is the friction coefficient and υ is the specific volume of the micelles in solution. As observed in Figure 3, the positive term in eq 10 is dominant, indicating that the mixed solvent is a good solvent for the block copolymers. Relating A_2 to the effective hard-sphere volume of the micelles, υ_{hs}, ($A_2 = 4N_A\upsilon_{hs}/M_w^2$)[38] it shows that the first term depends on the ratio υ_{hs}/M_w. Table 3 shows the estimation of A_2 values that were made taking the thermodynamics radius obtained from SLS data (see below). It can be observed that A_2 increases with the 1,4-dioxane concentration. This can be explained by considering that the main contribution to the A_2 value is that corresponding to the micelle core provided that the solvent mixtures with increasing amounts of dioxane show a larger solvent goodness for the micelle core. Thus, as the dioxane content increases, the micelle becomes softer due to the swelling of the hydrophobic SO chains. Table 3 also shows the hydrodynamic radii, r_h obtained through the intercepts of linear plots of the reciprocal of the intensity average of $r_{h,app}$ against concentration (see Figure 3). Note that through eq 1 the reciprocal of $r_{h,app}$ is proportional to $D_{app}/\eta T$ and so compensated for changes in solvent viscosity and temperature. The results indicate a reduction of r_h with 1,4-dioxane concentration attributed to the combination of the increase in solvent viscosity and a decrease in the aggregation

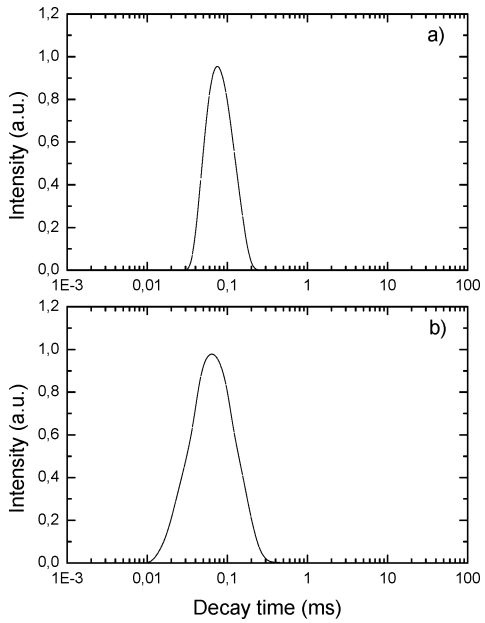

Figure 2. Decay time distributions of diblock $SO_{17}EO_{65}$ copolymer at a concentration of 60 g dm^{-3} in aqueous solution with a 1,4-dioxane content of (a) 5 (v/v) and (b) 35% (v/v) at 20 °C.

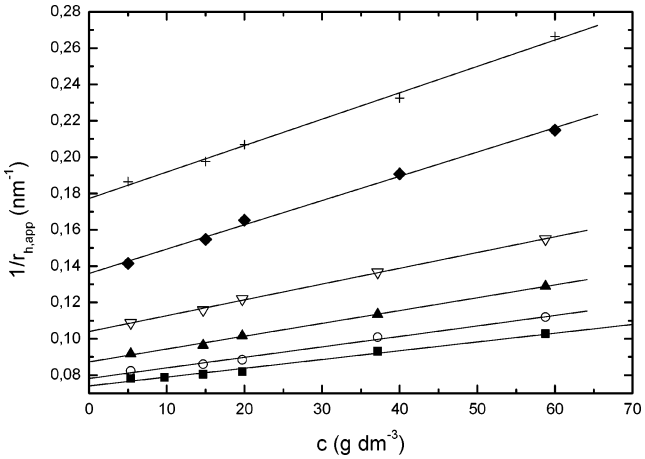

Figure 3. Concentration dependence of the reciprocal apparent hydrodynamic radii for micellar solutions of copolymer $SO_{17}EO_{65}$ at different compositions of the water−dioxane binary solvent: (■) 0, (○) 5, (▲) 15, (▽) 30, (◆) 45, and (+) 50% (v/v) at 20 °C.

TABLE 3: Micellar and Hydration Properties of Block Copolymer $SO_{17}EO_{65}$ in Different Aqueous−Dioxane Mixed Solvents at 20 °C

% (v/v)	A_2 (10^{-4} mol g^{-2} cm^3)	δ_t	M_w (10^5 mol g^{-1})	r_h (Nm)	N_w	r_t (nm)	r_c (nm)	ν_E (nm^3)	n_w
0	0.2	4.0	8.4	13.1	160	10.6	4.9	0.42	12
5	0.2	4.0	7.8	12.5	153	10.3	4.8	0.41	11
15	0.3	3.8	4.4	11.1	86	8.5	4.0	0.41	11
30	0.8	3.6	1.8	9.3	34	6.3	2.9	0.42	12
40	2.2	3.1	0.7	7.1	13	4.5	2.1	0.40	11
50	3.5	2.7	0.4	5.5	8	3.8	1.8	0.39	10

number or a decrease in overall micellar solvation. To solve this point, we have used static light scattering measurements.

For the present micellar solutions, the intensity dissymmetries for the scattering angles 45° and 135° (I_{45}/I_{135}) were 1.04 or less, which are consistent with micelles with small radius of gyration, r_g; a maximum value of $r_g \sim 9.8$ nm can be obtained from $r_g = 0.775r_h$ by treating the micelles as uniform spheres.

The Debye equation taken to the second term, A_2, could not be used to analyze the SLS data as micellar interactions cause curvature of the Debye plot across the concentration range investigated. This feature is illustrated in Figure 4, which shows the Debye plots for the copolymer at selected 1,4-dioxane concentrations in the mixed solvent. The fitting procedure used for the curves was based on scattering theory for hard spheres[39] whereby the interparticle interference factor (structure factor, S) in the scattering equation

$$K^*c/(I - I_s) = 1/SM_w \qquad (11)$$

was approximated by

$$1/S = [(1 + 2\phi)^2 - \phi^2(4\phi - \phi^2)]\,(1 - \phi)^{-4} \qquad (12)$$

where ϕ is the volume fraction of equivalent uniform spheres. Values of ϕ were conveniently calculated from the volume fraction of copolymer in the system by applying a thermodynamic expansion factor $\delta_t = \upsilon_t/\upsilon_a$, where υ_t is the thermodynamic volume of a micelle (i.e., one of eighth of the volume, u, excluded by one micelle to another) and υ_a is the anhydrous volume of a micelle ($\upsilon_a = \nu M_w/N_A$), where υ is the partial specific volume of the copolymer solute. The fitting parameter, δ_t, applies as an effective parameter for compact micelles irrespective of their exact structure. The method is equivalent to use the virial expansion for the structure factor of effective hard spheres taken to its seventh term[39] but requires just two adjustable parameters, i.e., M_w and δ_t. Values of these two quantities are shown in Table 3. In addition, weight-average association numbers, N_w, of the copolymer micelles in the mixed solvents were calculated from the micellar molecular mass derived from the fitting procedure shown above and the weight-average molecular weight of the copolymer in the unimer state (see Table 1).

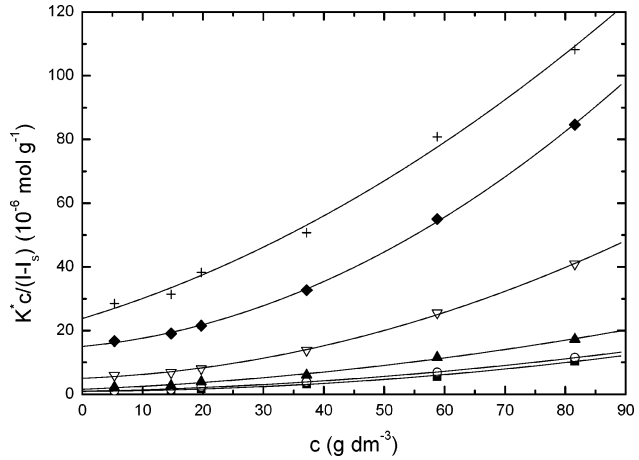

Figure 4. Debye plots for aqueous solutions of $SO_{17}EO_{65}$ at different 1,4-dioxane concentrations: (■) 0, (○) 5, (▲) 15, (▽) 30, (◆) 45, and (+) 50% (v/v) at 20 °C.

At this point, it is necessary to be reminded that a possible problem with light scattering is preferential absorption of one component of the binary solvent. When a polymer is dissolved in a binary solvent mixture, eqs 2 and 5 can still be used, but considering M_w and A_2 as apparent values.[40] Since water is a selective solvent for the SO blocks, it is expected that certain preferential adsorption of the hydrophobic blocks by dioxane molecules occurs whereas the EO blocks will not show any preference. In this regard, N_w values decrease as the 1,4-dioxane concentration in the solvent mixture increases, indicating that the mixed solvent becomes a better solvent for the polyoxystyrene blocks; that is, the micelle association number depends on the solvent quality in relation to the copolymer blocks that form the micelle core. Values of the equivalent hard-sphere radius (the thermodynamic radius, r_t) calculated from the thermodynamic volume of the micelles, i.e., from $\upsilon_t = \delta_t\upsilon_a$, are also listed in Table 3, confirming the reduction in micelle size.

In this regard, the polyoxystyrene insolubility in water promotes association into micelles, while interactions between PEO chains oppose it. The addition of dioxane counterbalances the possible partial deswelling of the EO chains due to the water content decrease and breakdown of their icelike structure, reduces the solvophobicity, and increases the solubility of the SO blocks, causing the lowering of the interfacial tension between the polyoxystyrene core and the solvent, favoring the swelling of hydrophobic blocks, as has been confirmed by compressibility measurements elsewhere.[16] Therefore, to achieve thermodynamic equilibrium, the micelle size should be smaller as the water content decreases, as seen in Table 3 for both hydrodynamic and thermodynamic radii. This size reduction originates mainly from the reduction in the aggregation number as the 1,4-dioxane concentration increases (see Table 3), which indicates that the mixed solvent becomes a better solvent for copolymer molecules, as previously noted. Similar behavior has been observed for other block copolymers.[41−43] From data in Table 3, it can be observed that the aggregation number of the block copolymer decreases by ∼95% whereas the hydrodynamic volume decreases by ∼71% at from 0 to 50% (v/v) 1,4-dioxane. This fact confirms that size reduction is prima rily lead by a decrease in aggregation number. Nevertheless, the swelling of the SO blocks implies that the size reduction is slightly less severe than the decrease in N_w.

On the other hand, taking the length of a SO unit to be 0.36 nm per chain unit,[38] the average length of the fully stretched SO_{17} block is 6.1 nm. The average core volume (ν_c) and core radius (r_c) can be estimated from the equation

$$\nu_c = (4/3)\pi r_c^3 = n\nu_S N_w \quad (13)$$

where ν_S is the volume of a SO unit

$$\nu_S = M_{w,S}/\rho_s N_A \quad (14)$$

with $M_{w,SO} = 120$ g mol^{-1} and $\rho_S = 1.13$ g cm^{-3} being the molar mass of a SO unit and the density of liquid oxystyrene, respectively, assuming spherical micelles cores with no penetration of water. Nevertheless, it has been demonstrated through SANS data that the amount of water in propylene and butylene oxide cores of block copolymers is ∼20−60% (v/v),[44−48] depending on solution conditions and the copolymer hydrophobicity. Therefore, it would be reasonable to expect that styrene oxide blocks should have smaller water core contents than propylene and butylene oxide block copolymers at room temperature, but some still present. Representative values of N_w of 165 for the block copolymer imply core radii of ∼4.9 nm, equivalent to fully stretched chains of length SO_{14}. Assuming that SO blocks have Poisson distributions, as expected in an ideal polymerization of an alkylene oxide,[38] and given the range of block lengths, we see that micelles should be spherical.

In addition, in accord with the assumption that micelles have a spherical structure with a liquidlike core[49] free of solvent molecules, we can further evaluate in a qualitative manner the extent of drainage of the micellar corona. From the reduction of the thermodynamic radius, r_t, *by* r_c, the thickness of the micellar corona is obviously derived, and, hence, the volume of each solvent-swollen EO unit, ν_E, can be derived from the relation

$$(4/3)\pi(r_t^3 - r_c^3) = mN_w\nu_E = \langle L_h \rangle \quad (15)$$

where L_h is the micellar corona thickness and ν_E the volume of each solvent swollen EO unit. Values of ν_E, Table 3, show that the block copolymer corona decreases its hydration very slightly as the 1,4-dioxane concentration in the mixed solvent increases. This requires that deswelling of the PEO chains is small due to the ability of 1,4-dioxane to form hydrogen bonds. In this regard, Raman spectroscopy has been used to show that there are six water molecules in the hydration shell of an EO unit: two H-bonded directly to the ether oxygen and four involved in hydrophobic hydration of the hydrophobic part of the unit.[50] The rest will be essentially bulk water, restricted to the corona to some extent, which is determined by the balance of osmotic and dynamic forces.

Temperature Influence on Micellar Behavior. It is known that polystyrene oxide−polyethylene oxide-based block copolymers show slight or null temperature dependence micellization as a consequence of the SO blocks that are tightly coiled in the dispersed molecular state, so that the interaction of a SO unit with water is much reduced in comparison with other hydrophobic blocks as PO or BO, which are much less hydrophobic (ratio of hydrophobicities in terms of cmc values PO:BO:SO = 1:6:12).[31] Presumably, the usually higher values of $\Delta_{mic}H°/n$ found for the triblock copolymers reflect a greater extension of their SO blocks resulting from the two EO blocks. In addition, the micellar aggregation number, N_w, slightly increases as the temperature rises since water becomes a poorer solvent for the unimers. As discussed elsewhere,[26,51] the onset of gelation in this type of copolymer and their increase at low temperature is associated with an increase in the extent of aggregation (i.e., an increase in the effective volume fraction of micelles in solution). The gel state is defined as the immobile fluid in the inversion tube test with yield stress $\sigma_y \geq 30$ Pa, and for spherical micelles packed in a cubic array as the present poly(styrene oxide)−poly(ethylene oxide) block copolymers, it is known that σ_y/G' with G measured at 1 Hz, which means a storage modulus for cubic hard gel of $G' \geq 1$ kPa. However, between the liquid micellar state and the gel state, there is a region where the micellar fluid does not behave either as a sol or a proper gel since it shows a low yield stress and a storage modulus larger than the loss modulus ($G' > G''$) but with $G' < 1$ kPa. This state is called soft gel (adopting the notation of Hvidt et al.[52]), and its boundaries in the complete block copolymer phase diagram have been typically defined by means of rheometry.

Figure 5 shows the scattered intensity relative to benzene obtained by SLS for copolymer $SO_{17}EO_{65}$ in the temperature range 20−90 °C and copolymer concentrations of 15 and 75 g dm^{-3}. From this figure, it can be observed that there is a temperature range where the scattered light intensity is almost constant and at a certain temperature the intensity starts to increase abruptly. For comparison, the scattered intensity of the triblock copolymer $EO_{67}SO_{15}EO_{67}$ at the same concentrations and temperature range has been also measured. Provided that both block copolymers are fully micellized at the concentrations measured, the change in intensity cannot be assigned to the existence of a cmt at which the copolymer begins to aggregate. Rheology measurements have shown that the boundary from the dilute liquid micellar state (or sol) to a soft gel state (or interacting liquid micellar state) occurs in a similar temperature range, so the inflection point can be correlated to this transition. Panels c and d in Figure 5 show the whole phase diagram of the present block copolymers obtained by tube inversion and rheology, in which the sol−soft gel transition boundary defined by both SLS and rheology fairly agrees as can be observed. As commented previously, soft gels display a detectable yield stress, a storage modulus significantly above the level characteristic of a sol (i.e., $G' > 10$ Pa at 1 Hz) with $G' > G''$ provided that a sol has a very low modulus and $G'' > G'$ (see Figure 5e as an example). Thus, it seems that SLS provides a quick method to determine this boundary.

The existence of the soft gel behavior is a consequence of the attraction of spherical micelles formed by these copolymers in water at temperatures where it becomes a poorer solvent for micelles. This is corroborated by the frequency scan for a 13% (w/v) solution of copolymer $EO_{67}SO_{15}EO_{67}$ at 50 °C, which has low values of G' (e.g., $G' \approx 20$ Hz at $f = 1$ Hz, $A = 0.5\%$) and with indications of a moduli crossover at low frequency, corresponding to a Maxwell fluid, at most, showing localized cubic order (see Figure 6). We hypothesize that the soft gel comprises a dynamic of weaking interacting spherical micelles and that the transition from sol to gel occurs when micellar aggregates with a fractal geometry reach a percolation threshold at critical micelle fraction ϕ_{sc} and so bridge the whole system.[53,54] The fact that the density of the water-swollen micelles is little different from water itself lends credence to this model. Soft gels of this type have been also identified in aqueous micellar solutions of other EO−SO,[17,55] EO−BO,[56,57] and EO−PO−EO Pluronic block copolymers.[52,58] In particular, Mallamace and co-workers have identified mechanisms of percolation and packing (structural arrest), depending on temperature and concentration in solutions of Pluronic copolymers.[59]

It is worth mentioning that a second type of soft gel can be formed at concentrated polymer solutions close to the sol−gel boundary, i.e., at concentrated copolymer solutions, due to defective ordered structures, which resembles the rheological behavior of the physical gels.[60] In addition, similar temperature

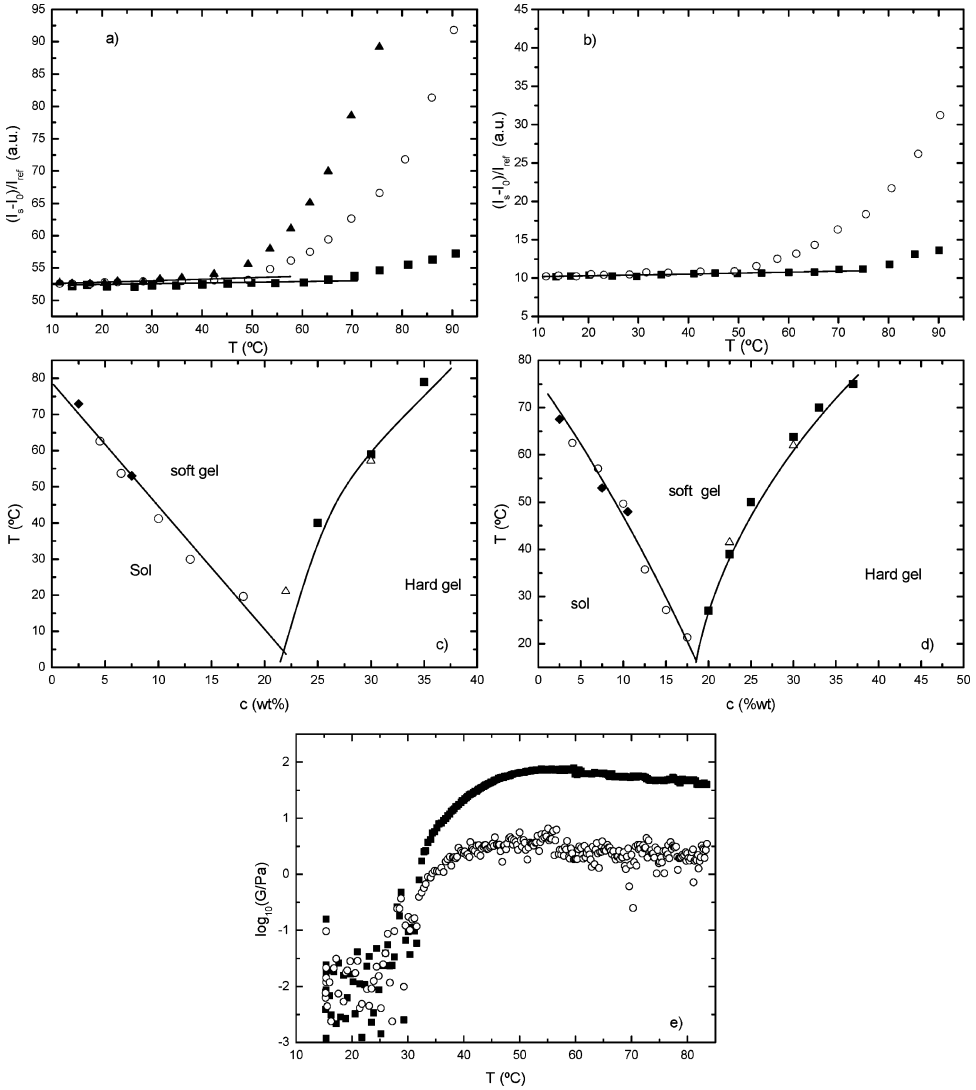

Figure 5. Scattered intensity at 90° of copolymers (a) $SO_{17}EO_{65}$ and (b) $EO_{67}SO_{15}EO_{67}$ in water at 20 °C. Partial gel boundaries of copolymers (from refs 17 and 55) (c) $EO_{67}SO_{15}EO_{67}$ and (d) $SO_{17}EO_{65}$ in aqueous solution from (■) tube inversion, (△, ○) rheometry, and (◆) SLS. Solid lines through the data points have no theoretical significance and are intended to guide the eye. (e) Temperature dependence of (■) storage (G') and (○) loss (G'') moduli of copolymer $EO_{67}SO_{15}EO_{67}$ at 13% (w/v), frequency $f = 1$ Hz, and strain $A = 0.5\%$.

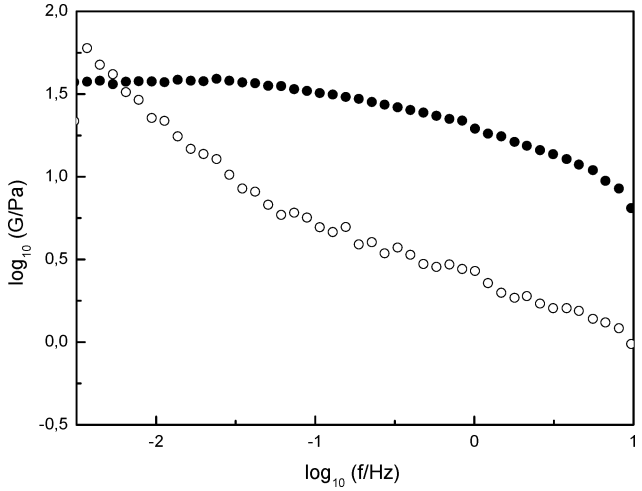

Figure 6. Frequency dependence of (■) storage (G') and (○) loss (G'') moduli of copolymer $EO_{67}SO_{15}EO_{67}$ at a concentration of 13% (w/v) at 50 °C (strain $A = 0.5\%$).

dependence of the static light scattering intensity has been found when the sphere to rod transition takes place at elevated temperature, as occurred for different Pluronic and PEO−PBO copolymers.[61,62] Nevertheless, this transition is not expected for our copolymers since these form compact spherical micelles tightly coiled in aqueous solution,[17,55] with a small temperature dependence of aggregation number (changes in ∼10 and ∼5 monomer units in a range of 25 °C). In this regard, the maximum aggregation number compatible with a spherical compact geometry according to eq 13 would be ∼330 and ∼70 for the diblock and triblock copolymers, respectively. Such high aggregation numbers are not probably reached in the light of the weak temperature dependence of N_w for both copolymers, so the sphere to rod transition will not take place.

On the other hand, from DLS measurements we have also observed changes in the field correlation function, $g_1(q,t)$ of copolymer upon heating. For a determined concentration, at low polymer concentration $g_1(q,t)$ could be modeled as an ergodic system of dilute diffusing monodisperse particles by fitting to a single-exponential function of the type

$$g_1(q,t) \approx \exp(-t/\tau_1) \tag{16}$$

where τ_1 is a characteristic decay time of the system (∼0.03 ms) associated to micellar diffusion of non-interacting micelles (see Figure 7a).[17,63]

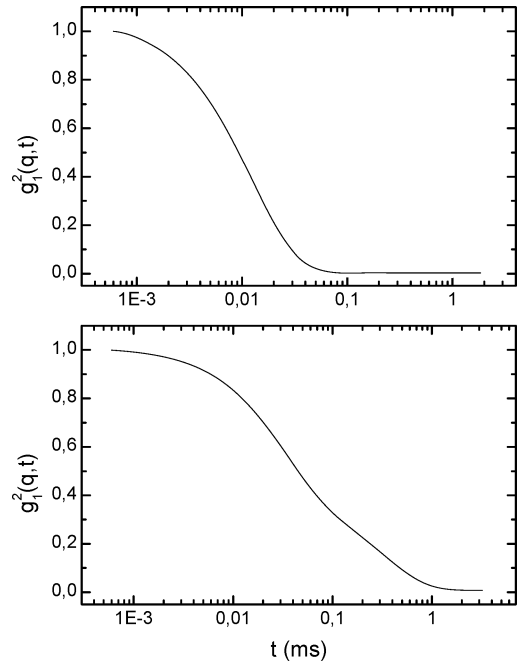

Figure 7. Selected correlation function at 90° of copolymer $SO_{17}EO_{65}$ (75 g dm^{-3}) at (a) 20 and (b) 55 °C.

However, at larger temperatures above the soft gel transition, it can be observed that for a fixed concentration $g_1(q,t)$ decays to zero at longer times and displays a very slight shoulder within the time range 0.1−1 ms. In addition, $g_1(q,t)$ cannot be fitted to a single exponential and was instead fitted to a sum of exponentials (see Figure 7b):

$$g_1(q,t) = A_0 + A_1 \exp(-t/\tau_1) + A_2 \exp(-t/\tau_2) \quad (17)$$

where τ_2 is a second characteristic time of the system (∼0.2−0.3 ms) and A_i are the relative scattering amplitudes of the system ($\Sigma_i A_i = 1$). A second characteristic mode has been also found for the correlation function of concentrated solutions of micelles (close to physical gelation) formed by PEO−PBO copolymer solutions, for example,[47,63] associated with nondiffusive phenomena as a consequence of the sufficient local packing of micelles to form a continuous stress-bearing network supported by short-time contacts between EO chains of adjacent micelles. Other copolymers with different architecture, such as PS−EB−PS and BO−EO−BO triblock copolymers, also display this type of mode associated, in this case, with the formation of loops or bridges between adjacent micelles.[64,65] In our case, although our copolymer concentrations are still far from the critical gel concentration (∼200 and ∼240 g dm^{-3} for the diblock and triblock copolymers, respectively) it seems that the interaction between copolymer micelles is already sufficient to denote certain collective behavior due to the interacting spherical micelles, once the sphere-to-rod transition is not possible, as commented on previously. In addition, this behavior also resembles that displayed by microemulsions near the percolation transition, where two relaxation modes correspond to collective diffusion (fast mode) and self-diffusion (slow mode).[66] Additional studies are being carried out in both this dilute regime and the concentrated regime next to the critical gelation concentration in order to gain additional information on the dynamics of these systems and to elucidate the similarities and differences between the different regimes, which will be reported elsewhere.

Conclusions

In this work, we have analyzed how the presence of 1,4-dioxane affects the surface and micellar properties of the block copolymer $SO_{17}EO_{65}$. Surface tension data have shown that the cmc values increase as the 1,4-dioxane content in the binary solvent does. The surface parameters show that the presence of the cosolvent involves the necessity of a larger space in the interface for the copolymer molecule. From light scattering data, it can be observed that both hydrodynamic radii and micellar aggregation number decrease as the concentration of 1,4-dioxane in the solvent increases. The increasing amounts of 1,4-dioxane reduce the solvophobicity of the SO blocks since it is a good solvent and thus increases their solubility in solution. As a consequence, a reduction in the interfacial tension between the micellar core composed by SO blocks and the solvent occurs, favoring the swelling of the hydrophobic blocks. Thus, to achieve thermodynamic equilibrium, the micelle size must be smaller. From a simple modelization, it is determined that the extent of the corona hydration by water molecules slightly decreases with the dioxane content. On the other hand, static light scattering measurements have been proven to be a simple method to get reliable data of the lower boundaries of the transition between a liquid micellar solution and a soft micellar gel formed by interacting spherical micelles with collective behavior upon heating. Comparison of the transition temperatures derived from SLS and rheology for micellar solutions of copolymers $SO_{17}EO_{65}$ and $EO_{67}SO_{15}EO_{67}$ show a good agreement. In addition, changes in the autocorrelation function obtained from dynamic light scattering are also observed related to the appearance of a second relaxation mode corresponding to local micellar clusters.

Acknowledgment. The authors thank Ministerio de Educación y Ciencia (MEC) through projects MAT2007-61604 and, and Xunta de Galicia for financial support. S.B. also thanks MEC for her Juan de la Cierva position and E.C. for his postdoctoral scholarship.

References and Notes

(1) Tuzar, Z.; Kratochvil, P. *Surface and Colloid Science*; Plenum Press: New York; 1993; Vol. 15.
(2) Alexandridis, P., Lindman, B. Eds. *Amphiphilic Block Copolymers: Self-Assembly and Applications;* Elsevier Science, B. V.: Amsterdam, 2000.
(3) Chu, B.; Zhou, Z. Physical Chemistry of Polyoxyalkylene Block Copolymer Surfactants. In *Nonionic Surfactants*; Nace, V. M., Ed.; Surfactant Science Series; Marcel Dekker; New York, 1996.
(4) Kwak, J. C. T. *Polymer-Surfactant Systems;* Surfactant Science Series 77; Marcel Dekker: New York, 1998.
(5) Wanka, G.; Hoffmann, H.; Ulbritch, W. *Macromolecules* **1994**, *27*, 4145.
(6) Förster, S.; Antonietti, M. *Adv. Mater.* **1998**, *10*, 195.
(7) Amstrong, J.; Chowdhry, B.; Mitchell, J.; Beezer, A.; Leharne, S. *J. Phys. Chem.* **1996**, *100*, 1738.
(8) Alexandridis, P.; Holzwarth, J. F. *Langmuir* **1997**, *13*, 6074.
(9) Ma, J.-H.; Guo, C.; Tang, Y. L.; Wang, J.; Zheng, L.; Liang, X.-F.; Chen, S.; Liu, H.-Z. *Langmuir* **2007**, *23*, 3075.
(10) Cheng, Y.; Jolicoeur, C. *Macromolecules* **1995**, *28*, 2665.
(11) Alexandridis, P.; Yang, L. *Macromolecules* **2000**, *33*, 5574.
(12) Ivanova, R.; Lindman, B.; Alexandridis, P. *Adv. Colloid Interface Sci.* **2001**, *89*−*90*, 351.
(13) Svensson, B.; Olsson, U.; Alexandridis, P. *Langmuir* **2002**, *16*, 6839.
(14) Holmquist, P.; Alexandridis, P.; Lindman, B. *Langmuir* **1997**, *13*, 2471.
(15) Kelarakis, A.; Havredaki, V.; Booth, C. *Macromol. Chem. Phys.* **2004**, *205*, 1594.
(16) Castro, E.; Taboada, P.; Mosquera, V. *J. Phys. Chem. B* **2006**, *110*, 13113.
(17) Crothers, M.; Attwood, D.; Collett, J. H.; Yang, Z.; Booth, C.; Taboada, P.; Mosquera, V.; Ricardo, N. P. S.; Martini, L. G. A. *Langmuir* **2002**, *18*, 8685.

(18) Castro, E.; Taboada, P.; Mosquera, V. *J. Phys. Chem. B* **2004**, *108*, 3030−3035.
(19) Shen, H.; Eisenberg, A. *J. Phys. Chem. B* **1999**, *103*, 9473.
(20) Choucair, A.; Lavigueur, C.; Eisenberg, A. *Langmuir* **2004**, *20*, 3894.
(21) Yu, K.; Eisenberg, A. *Macromolecules* **1996**, *29*, 6359.
(22) Yu, K.; Eisenberg, A. *Macromolecules* **1998**, *31*, 3509.
(23) Wu, J.; Eisenberg, A. *J. Am. Chem. Soc.* **2006**, *128*, 2880.
(24) Seo, M.-H.; Choi, I.-J. PCT Int. Application, 2001.
(25) Kang, H. R. *J. Imaging Sci.* **1991**, *35*, 179.
(26) Rekatas, C. J.; Mai, S.-H.; Crothers, M.; Quinn, M.; Collet, J. H.; Attwood, D.; Heatley, F.; Martini, L.; Booth, C. *Phys. Chem. Chem. Phys.* **2001**, *3*, 4769.
(27) Provencher, S. W. *Makromol. Chem.* **1979**, *180*, 201.
(28) Gulari, E.; Chu, B. *Biopolymers* **1999**, *32*, 2943.
(29) Huglin, M. B. *Light Scattering from Polymer Solutions;* Plenum Press: New York, 1972.
(30) Mai, S.-M.; Ludhera, S.; Heatley, F.; Attwood, D.; Booth, C. *J. Chem. Soc. Faraday Trans.* **1998**, *94*, 567. Mai, S.-M.; Booth, C.; Kelarakis, A.; Havredaki, V.; Ryan, A. J. *Langmuir* **2000**, *16*, 1681.
(31) Booth, C.; Attwood, D:; Price, C. *Phys. Chem. Chem. Phys.* **2006**, *8*, 3612.
(32) Tamakaku, T.; Yamaguchi, A.; Tabata, M.; Nishi, N.; Yoshida, K.; Wakita, H.; Yamaguchi, T. *J. Mol. Liq.* **1999**, *83*, 163.
(33) Wu, Y. G.; Tabata, M.; Takamaku, T. *J. Mol. Liq.* **2001**, *94*, 273.
(34) Rosen, J. M.; Cohen, A. W.; Dahanakaye, M.; Hua, X. *J. Phys. Chem.* **1982**, *86*, 541.
(35) Sultana, S. B.; Bhat, S. G. T.; Rakshit, A. K. *Langmuir* **1997**, *13*, 4562.
(36) Marcus, Y. *Ion Solvation*; Wiley: London, 1985.
(37) Vink, H. *J. Chem. Soc., Faraday Trans. 1* **1985**, *81*, 1725.
(38) Flory, P. J., *Principles of Polymer Chemistry*; Cornell UP: Ithaca, NY, 1953; p 532. For spheres, the excluded volume is eight times the hard-sphere volume.
(39) Percus, J. K.; Yevick, G. J. *J. Phys. Rev.* **1958**, *110*, 1. Vrij, A. *J. Chem. Phys.* **1978**, *69*, 1742. Carnahan, N. F.; Starling, K. E. *J. Chem. Phys.* **1969**, *51*, 635.
(40) Solomon, M. J.; Müller, S. J. *J. Polym. Sci., Part B: Polym. Phys.* **1996**, *34*, 181.
(41) Wu, G.; Zhou, Z.; Chu, B. *Macromolecules* **1993**, *26*, 2117.
(42) Alexandridis, P.; Yang, L. *Macromolecules* **2000**, *33*, 5574.
(43) Villacampa, M.; Díaz de Apodaca, E.; Quintana, J. R.; Katime, I. *Macromolecules* **1995**, *28*, 4144.
(44) Goldmints, I.; von Gottberg, F. K.; Smith, K. A.; Hatton, T. A. *Langmuir* **1997**, *13*, 3659.
(45) Liu, Y.; Chen, S. H.; Huang, J. S. *Macromolecules* **1998**, *31*, 2236.
(46) Pedersen, J. S.; Gerstenberg, M. C. *Colloids Surf. A* **2003**, *213*, 175.
(47) Castelletto, V.; Hamley, I. W. *J. Chem. Phys.* **2002**, *117*, 8124.
(48) Castelletto, V.; Hamley, I. W. *Langmuir* **2004**, *20*, 2992.
(49) Zhou, Z-K; Chu, B. *J. Colloid Interface Sci.* **1988**, *126*, 171.
(50) Goutev, N.; Nickolov, Z. S.; Georgiev, G.; Matsura, H. *J. Chem. Soc., Faraday Trans.* **1997**, *93*, 3167−3171.
(51) Kelarakis, A.; Havredaki, V.; Yuan, X.-F.; Chaibundit, C.; Booth, C.; *Macromol. Chem. Phys.* **2006**, *207*, 903.
(52) Hvidt, S.; Jørgensen, E. B.; Brown, W.; Schillén, K. *J. Phys. Chem.* **1994**, *98*, 12320.
(53) Li, H.; Yu, G.-E.; Price, C.; Booth, C.; Hech, E.; Hoffmann, H. *Macromolecules* **1997**, *30*, 1347.
(54) Dickenson, E.; Elvington, C.; Euston, S. R. *J. Chem. Soc., Faraday Trans. 2*, **1989**, *85*, 891.
(55) Yang, Z.; Crothers, M.; Ricardo, N. M. P. S.; Chaibundit, C.; Taboada, P.; Mosquera, V.; Kelarakis, A.; Havredaki, V.; Martini, L.; Valder, C.; Collett, J. H.; Attwood, D.; Heatley, F.; Booth, C. *Langmuir* **2003**, *19*, 943.
(56) Chaibundit, C.; Sumanatrakool, P.; Chinchew, S.; Kanatharana, P.; Tattershall, C.; Booth, C.; Yuan, X.-F. *J. Colloid Interface Sci.* **2005**, *283*, 544.
(57) Li, H.; Yu, G.-E.; Price, C.; Booth, C.; Fairclough, J. P. A.; Ryan, A. J.; Mortensen, K. *Langmuir* **2003**, *19*, 1075.
(58) Mortensen, K.; Perdersen, J. K. *Macromolecules* **1993**, *26*, 805.
(59) Chen, S. H.; Chen, W. R.; Mallamace, F. *Science* **2003**, *300*, 619.
(60) Castelletto, V.; Hamley, I. W.; Crothers, M.; Attwood, D.; Yang, Z.; Booth, C. *J. Macromol. Sci. Phys.* **2004**, *43*, 13.
(61) Schillén, K.; Brown, W.; Johnsen, R. M. *Macromolecules* **1994**, *27*, 4825.
(62) Chaibundit, C.; Sumanatrakool, P.; Chinchew, S.; Kanatharana, P.; Tattershall, C. E.; Booth, C.; Yuan, X.-F. *J. Colloid Interface Sci.* **2005**, *283*, 544.
(63) Castelletto, V.; Hamley, I. W. *J. Chem. Phys.* **2004**, *121*, 11474.
(64) Konak, C.; Fleischer, G.; Tuzar, Z.; Bansil, R. *J. Polym. Sci. Part B: Polym. Phys.* **2000**, *38*, 1312.
(65) Mistry, D.; Annable, T.; Yuan, X.-F.; Booth, C. *Langmuir* **2006**, *22*, 2986.
(66) Shulka, A.; Graener, H.; Neubert, R. H. H. *Langmuir* **2004**, *20*, 8526.